GENERAL MODEL FOR AIRBORNE AND SPACEBORNE LINEAR ARRAY SENSORS

Daniela Poli

Institute of Geodesy and Photogrammetry, Swiss Federal Institute of Technology, Zurich, Switzerland
daniela@geod.baug.ethz.ch

KEY WORDS: Orientation, Modelling, GPS/INS, Integration, Triangulation, Three-Line

ABSTRACT

This paper describes a general model for CCD linear array sensors with along-track stereo viewing. The sensor external orientation, which is different for each image line, is modelled with time-dependent piecewise polynomial functions and integrated in the standard photogrammetric triangulation, resulting in an indirect georeferencing model. The continuity of the functions and their first and second derivatives between adjacent segments is imposed. In case of sensors carried on airplane, the sensor position and attitude observed by GPS/INS instruments are included in the piecewise polynomial functions. Using Ground Control Points (GCPs) and, additionally, Tie Points (TPs), the function parameters and the ground coordinates of the TPs are estimated in a least-squares adjustment.

The model was tested on imagery acquired by TLS and MOMS-02 sensors, which were carried on helicopter and satellite respectively, using different numbers and distributions of GCPs. The Japanese TLS (Three-Line Sensor) scans along-track in 3 directions with a one-lens optical system. The sensor external orientation for each image line was available by GPS/INS instruments, together with 46 GCPs measured in the images. An absolute accuracy of 4-13 cm in planimetry and 6-16 cm in height was achieved (ground pixel size: 10 cm).

MOMS-02 sensor was carried on the Russian MIR station. The stereopairs used for the test were acquired during the Priroda mission in 1997 and had ground resolution of 18m. The preliminary results showed an absolute accuracy of 6.3-9.3 m in planimetry and 3.0-12.3 m in height.

1. INTRODUCTION

Today linear CCD array sensors are widely used to acquire panchromatic and multispectral imagery in pushbroom mode for photogrammetric and remote sensing applications. Linear scanners are carried on aircraft (e.g. ADS40, DPA and WAAC from DLR, AirMISR from NASA), helicopter (e.g. TLS from STARLABO) or spacecraft (e.g. SPOT from CNES, IRS from ISRO, MISR and ASTER from NASA, IKONOS from SpaceImage, WAOSS from DLR) and allow photogrammetric mapping at different scales.

The stereoscopy of the images is achieved across- or along- the flight direction. Sensors with across-track stereo capability are in most cases carried on spacecraft (SPOT, IRS) and combine one linear CCD array perpendicular to the flight direction with a rotating mirror. Stereopairs are acquired from different orbits with a time delay in the order of days. On the other hand, sensors with along-track stereo capability scan the terrain surface with CCD arrays placed parallel to each other, perpendicular to the flight direction and inclined with different viewing angles along the trajectory. A very common geometry used both on airborne (ADS40, TLS, DPA, WAAC) and satellite (MOMS-02, WAOSS) in based on three lines looking forward, nadir and backward the flight direction. The advantage of the along-track stereo geometry over the across-track one is to enable the acquisition of a larger number of images with a smaller time delay. Within pushbroom sensors with along-track stereo viewing, the number of lenses is variable: some sensors (ADS40, TLS, DPA, WAAC, WAOSS) contain one lens common for all the CCD arrays, others (AirMISR, MISR) have one lens for each group of CCD lines looking in the same direction.

The images provided by linear CCD array sensors consist of lines scanned independently at different instants of time and stored one next to the other. Therefore each line of one image is acquired with a different set of values for the sensor position and attitude. In order to georeference this kind of imagery, a classic bundle adjustment is not realistic, because the number of unknowns (6 external orientation parameters for each image line) would be huge. Therefore an external orientation modelling is required.

In case of sensors carried on satellites, the exterior orientation can be modelled with functions depending on time, because the trajectory is quite smooth and predictable and the correlation between the orientation parameters is high. Third order Lagrange polynomials (Ebner et al., 1992; Kornus, 1998) and quadratic functions (Kratky, 1989) have already been proposed for this scope; the physical properties of the satellite orbit can also be included as constraints.

For airborne applications, where the trajectory is not predictable, the direct measurement of the external orientation is indispensable for the georeferencing of images acquired by linear scanners. Thanks to the successful improvement and rapid diffusion of positioning systems and data processing algorithms, nowadays GPS and INS systems provide precise position and attitude observations for direct georeferencing and image rectification (Haala et al., 1998; Cramer et al., 2000; Mostafa et al., 2000; Tempelmann et al., 2000). The position and attitude measured by GPS/INS do not refer to the perspective centre of the cameras, but to additional reference systems centred in the instruments themselves. The offset vectors and misalignment angles between the systems must be estimated with post-flight calibration procedures. In addition, the GPS/INS observations can also be affected by systematic errors. Therefore for high precision applications the errors and ambiguities contained in the GPS/INS data have to be modelled and integrated in the bundle adjustment of the imagery, resulting in an indirect georeferencing model (Lee et al., 2000; Chen, 2001; Gruen et al., 2002).

In this paper a general model for the georeferencing of multi-line CCD array sensors with along stereo viewing is presented. After a description of the general principles of georeferencing, the proposed approach for trajectory modelling and integration of GPS/INS observations will be described. The experimental results obtained testing the sensor model on MOMS-02 and TLS (Three-Line Sensor) imagery will be reported and discussed. The conclusions and planned work on the sensor model improvement will close the paper.

2. GEOREFERENCING OF MULTI-LINE SENSORS IMAGERY

The aim of georeferencing is to establish a relationship between image and ground reference systems, according to the sensor geometry and the available data. The image system is centred in the lens perspective centre (PC), with *x*-axis tangent to the flight trajectory, *z*-axis parallel to the optical axis and pointing upwards and *y*-axis along the CCD line, completing a right-hand coordinate system (Figure 1).

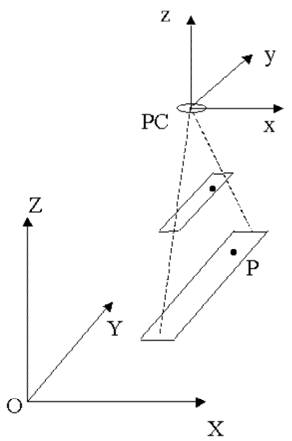

Figure 1. Image coordinate system with origin in instantaneous perspective centre (PC) and ground coordinate system with origin in O.

In case of CCD linear array scanners with along-track stereo capability, each image line is the result of a nearly parallel projection in the flight direction and a perspective projection in the CCD line direction. For each observed point, the relationship between image and ground coordinates is described by:

$$\begin{bmatrix} X \\ Y \\ Z \end{bmatrix} = \begin{bmatrix} X_C \\ Y_C \\ Z_C \end{bmatrix} + kR(\omega_C, \varphi_C, \kappa_C) \begin{bmatrix} x \\ y \\ -f \end{bmatrix} \qquad (1)$$

where:

$[X \ Y \ Z]$: point coordinates in the ground system;
$[X_C \ Y_C \ Z_C]$: PC position in the ground system;
$[x \ y \ -f]$: point coordinates in the image system;
f: focal length;
k: scale factor;
$R(\omega_C, \varphi_C, \kappa_C)$: rotation matrix from image to ground system, according to attitude angles $\omega_C, \varphi_C, \kappa_C$.

Solving Equation 1 with respect to x and y, the collinearity equations:

$$x = -f \cdot \frac{r_{11}(X-X_C) + r_{21}(Y-Y_C) + r_{31}(Z-Z_C)}{r_{13}(X-X_C) + r_{23}(Y-Y_C) + r_{33}(Z-Z_C)}$$
$$y = -f \cdot \frac{r_{12}(X-X_C) + r_{22}(Y-Y_C) + r_{32}(Z-Z_C)}{r_{13}(X-X_C) + r_{23}(Y-Y_C) + r_{33}(Z-Z_C)} \qquad (2)$$

are obtained.

For sensors whose optical systems consist of more lenses, additional geometric parameters describing the relative position and attitude of each lens with respect to the nadir one are imported in the collinearity equations (Ebner, 1992). Calling f_j the focal length, Δx_j, Δy_j, Δz_j the relative position and α_j, β_j, γ_j the relative attitude of each lens j, Equation 1 is extended to:

$$\begin{bmatrix} X \\ Y \\ Z \end{bmatrix} = \begin{bmatrix} X_C \\ Y_C \\ Z_C \end{bmatrix} + D(\omega_C, \varphi_C, \kappa_C) \begin{bmatrix} \Delta x_j \\ \Delta y_j \\ \Delta z_j \end{bmatrix} + kR(\omega_C, \varphi_C, \kappa_C, \alpha_j, \beta_j, \gamma_j) \begin{bmatrix} x \\ y \\ -f_j \end{bmatrix} \qquad (3)$$

where:

$M(\alpha_j, \beta_j, \gamma_j)$: rotation from image system centred in the off-nadir lens j to image system with origin in the central lens;
$D(\omega_C, \varphi_C, \kappa_C)$: rotation from image system centred in the central lens to ground frame.

$R = D(\omega_C, \varphi_C, \kappa_C) M(\alpha_j, \beta_j, \gamma_j)$: complete rotation from image system centred in the off-nadir lens j to ground frame.

The collinearity equations obtained from Equation 3 are:

$$x = -f_j \cdot \frac{r_{11}(X-X_C) + r_{21}(Y-Y_C) + r_{31}(Z-Z_C) - (m_{11}\Delta x_j + m_{21}\Delta y_j + m_{31}\Delta z_j)}{r_{13}(X-X_C) + r_{23}(Y-Y_C) + r_{33}(Z-Z_C) - (m_{13}\Delta x_j + m_{23}\Delta y_j + m_{33}\Delta z_j)}$$
$$y = -f_j \cdot \frac{r_{12}(X-X_C) + r_{22}(Y-Y_C) + r_{32}(Z-Z_C) - (m_{12}\Delta x_j + m_{22}\Delta y_j + m_{32}\Delta z_j)}{r_{13}(X-X_C) + r_{23}(Y-Y_C) + r_{33}(Z-Z_C) - (m_{13}\Delta x_j + m_{23}\Delta y_j + m_{33}\Delta z_j)} \qquad (4)$$

If the relative orientation parameters are equal to zero (nadir case), Equations 1 and 2 are obtained from Equations 3 and 4. The algorithms that will be presented have been developed both for one-lens and multi-lens CCD linear sensors.

Assuming that the focal lengths and the additional parameters are known, in order to solve Equations 1 and 3, six external orientation parameters (position, attitude) are required for each exposure. Therefore using Ground Control Points (GCPs) and Tie Points (TPs), a bundle adjustment for the external orientation and ground coordinates estimation is not realistic, because the number of unknown would be too large. For this reason the main problem for CCD linear scanners georeferencing is to include in the triangulation a suitable time-dependent function that models the exterior orientation and takes into account any additional information about the sensor position and attitude.
In the next section a general sensor model that integrates the external orientation model into the collinearity equations will be presented.

3. TRAJECTORY MODELLING

The sensor external orientation is modelled by piecewise polynomial functions depending on time.

The platform trajectory is divided into segments according to the number and distribution of available GCPs and TPs. For each segment i, with time extremes t^i_{ini} and t^i_{fin}, the variable $\bar{t}$ is defined as:

$$\bar{t}=\frac{t-t^i_{ini}}{t^i_{fin}-t^i_{ini}}\in[0,1] \tag{5}$$

being t the sensor exposure time.

Then in each segment the sensor external orientation (X_C, Y_C, Z_C, ω_C, φ_C, κ_C) is modelled with second-order polynomials depending on $\bar{t}$:

$$\begin{aligned}
X_C(\bar{t})&=X^i_0+X^i_1\bar{t}+X^i_2\bar{t}^2\\
Y_C(\bar{t})&=Y^i_0+Y^i_1\bar{t}+Y^i_2\bar{t}^2\\
Z_C(\bar{t})&=Z^i_0+Z^i_1\bar{t}+Z^i_2\bar{t}^2\\
\omega_C(\bar{t})&=\omega^i_0+\omega^i_1\bar{t}+\omega^i_2\bar{t}^2\\
\varphi_C(\bar{t})&=\varphi^i_0+\varphi^i_1\bar{t}+\varphi^i_2\bar{t}^2\\
\kappa_C(\bar{t})&=\kappa^i_0+\kappa^i_1\bar{t}+\kappa^i_2\bar{t}^2
\end{aligned} \tag{6}$$

where $[X_0 X_1 X_2 \ \dots \ \kappa_0\kappa_1\kappa_2]^i$ are the parameters modelling the external orientation in segment i.

At the points of conjunction between adjacent segments, constraints on the zero, first and second order continuity are imposed on the trajectory functions: we force that the values of the functions and their first and second derivatives computed in two neighbouring segments are equal at the segments boundaries. As the point on the border between segment i and $i+1$ has $\bar{t}=1$ in segment i and $\bar{t}=0$ in segment $i+1$, applying the zero order continuity for X_C function, we obtain:

$$X^i_C\Big|_{\bar{t}=1}=X^{i+1}_C\Big|_{\bar{t}=0} \tag{7}$$

It yields to:

$$X^i_0+X^i_1+X^i_2=X^{i+1}_0 \tag{8}$$

Similarly, imposing the first and second order continuity constraints for X_C function, we get:

$$\frac{dX^i_C}{d\bar{t}}\bigg|_{\bar{t}=1}=\frac{dX^{i+1}_C}{d\bar{t}}\bigg|_{\bar{t}=0} \tag{9}$$

and

$$\frac{d^2X^i_C}{d\bar{t}^2}\bigg|_{\bar{t}=1}=\frac{d^2X^{i+1}_C}{d\bar{t}^2}\bigg|_{\bar{t}=0} \tag{10}$$

They yield to:

$$X^i_1+2X^i_2=X^{i+1}_1 \tag{11}$$

for the first order derivative and to:

$$X^i_2=X^{i+1}_2 \tag{12}$$

for the second order one.

In the same way, equations 8, 11 and 12 are written for Y_C, Z_C, ω_C, φ_C and κ_C functions and are treated as soft (weighted) constraints.

3.1 Mathematical solution

The functions modelling the external orientation (Equation 6) are integrated into the collinearity equations (Equations 2 or 4), resulting in an indirect georeferencing model.

The collinearity equations are linearized with the first-order Taylor decomposition with respect to the unknown parameters modelling the sensor external orientation (x_{EO}), according to Equations 2 (or 4) and 6, and with respect to the unknown ground coordinates of the TPs (x_{TP}), according to Equations 2 or 4.

The initial approximations for the parameters modelling the sensor external orientation (x^0_{EO}) are provided by additional sources. In case of sensors carried on satellite, ephemeris from sophisticated orbit models and satellite-tracking systems give approximations on the spacecraft position, while INS instruments carried on board provide both the position and the attitude. If none of these data sources is available, approximations for the sensor position and attitude can be computed according to the orbit characteristics. As sensors carried on aircraft are concerned, approximations for the sensor external orientation are available only from GPS/INS instruments carried on board.

The initial values for the ground coordinates of the TPs (x^0_{TP}) are estimated with forward intersection, using the rough external orientation.

Combining the observations equations and the constraints, the system:

$$\begin{cases}
-e_{GCP}=A_{GCP}\,x_{EO} & -l_{GCP}\,;P_{GCP}\\
-e_{TP}=A_{TP}\,x_{EO}+B_{TP}\,x_{TP} & -l_{TP}\,;P_{TP}\\
-e_{C0}=C_0\,x_{EO} & -l_{C0}\,;P_{C0}\\
-e_{C1}=C_1\,x_{EO} & -l_{C1}\,;P_{C1}\\
-e_{C2}=C_2\,x_{EO} & -l_{C2}\,;P_{C2}
\end{cases} \tag{13}$$

is formed, where:

- x_{EO}: vector containing increments to x^0_{EO};
- x_{TP}: vector containing increments to x^0_{TP};
- A_{GCP}: design matrix for x_{EO} for GCPs observations;
- A_{TP}: design matrix for x_{EO} for TPs observations;
- B_{TP}: design matrix for x_{TP} for TPs observations;
- C_0, C_1, C_2: design matrices for constraints on zero, first and second order continuity;

e: observation errors;
l: discrepancy vectors;
P: weight matrices for each group of observations.

GCPs and TPs are required in order to solve the system and estimate the unknown external orientation parameters and TPs ground coordinates.

Considering a sensor with S linear CCD arrays, N_{GCP} GCPs, N_{TP} TPs and n_s trajectory segments, the complete system contains $2\text{x}S\text{x}(N_{GCP}+N_{TP})$ collinearity equations, together with $6\text{x}(n_s\text{-}1)$ equations for each group of constraints described in Equations 8, 11 and 12. The unknowns are $18\text{x}n_s$ for the external orientation and $3\text{x}N_{TP}$ for the TP ground coordinates. The vectors x_{EO} and x_{TP} are estimated with least-squares adjustment and added to x^0_{EO} and x^0_{TP} in the next iteration. The process stops when x_{EO} and x_{TP} are smaller than suitable thresholds.

4. TEST ON MOMS-02

The indirect georeferencing model was tested on a stereopair acquired by a CCD linear array sensor carried on spacecraft. The sensor was the German MOMS-02, mounted on the Russian MIR station. The images were taken over South Germany on March 14th, 1997, during the Priroda mission, from a height of approximately 400 km. MOMS-02 was a three-line sensor, with along-track stereo viewing provided by a high resolution nadir-looking lens (channel 5, 660 mm focal length) and two off-nadir lenses, looking forward (channel 6, +21.4 degrees, 237.25 mm focal length) and backward (channel 7, -21.4 degrees, 237.25 mm focal length) the MIR trajectory (Kornus, 1998).

The two images used in this work were taken from channel 6 and channel 7, with a time delay of 40 seconds and a ground resolution of 18 m (Figure 2). The nadir image could not be used because channel 5 on Priroda was defocused. Each image has a dimension of 2976 pixels across-track and 5736 pixels along-track and consists of a combination of two overlapping scenes (scenes 25-26) in the flight direction. Approximations of MIR orbit (high precision ephemeris) and attitude (INS measurements) for the periods of acquisition of the two test scenes were kindly provided by DLR.

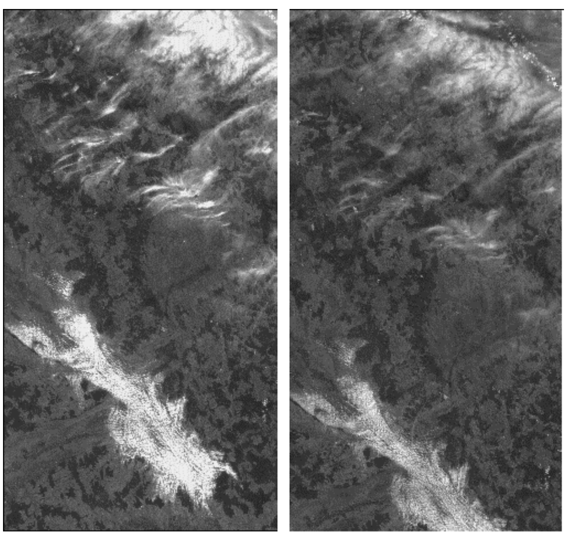

Figure 2. MOMS-02 stereo images from channel 6 (left) and channel 7 (right) after contrast enhancement and radiometric equalisation.

29 GCPs in regions free from clouds were acquired from a 1:50000 digital topographic map in Gauss-Krueger coordinate system; then they were manually measured in the left image and transferred to the other one with semi-automatic least-squares matching. Figure 3 shows the distribution of the 29 GCPs and the spacecraft trajectory.

4.1 Preliminary results

The general indirect georeferencing model was applied in order to estimate the parameters modelling the sensor external orientation and the ground coordinates of the TPs. As two distinct lenses acquired the stereopair, the collinearity equations for multi-lens sensors (Equation 4) were used. The values of the additional parameters describing the relative orientation between the lenses are concerned were available from (Ebner et al., 1992).

The GCPs coordinates and the spacecraft were transformed into the geocentric Cartesian system. From the available 29 object points, a group of them was used as GCPs and the remaining as TPs. The estimated coordinates of the TPs were compared to the correct ones and used for the results' control. The spacecraft trajectory was divided into different number of segments (1, 2 and 4) and 6, 10 and 15 GCPs were used as ground information. Taking into account the ground accuracy achieved and the minimum number of GCPs required, the best choice for the number of trajectory segments was 2. With this configuration, RMS of 9.374 m in X, 7.136 m in Y and 12.347 m in Z (ground pixel size: 18 m) were obtained with 10 GCPs. These results correspond to about 0.2, 0.4 and 0.7 times the pixel size.

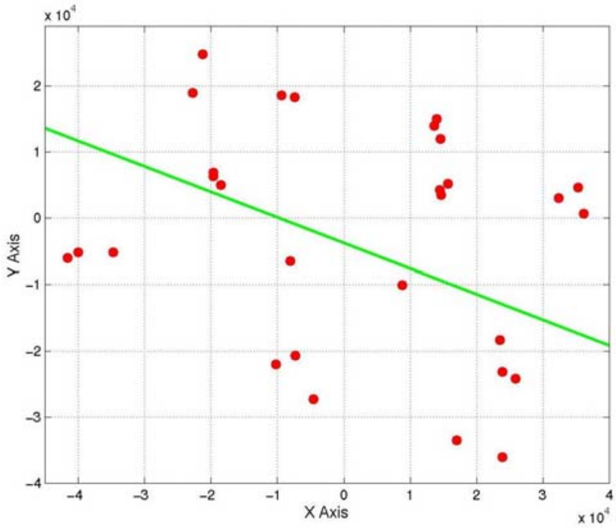

Figure 3. Spacecraft trajectory and distribution of GCPs in a local system.

5. INTEGRATION OF GPS/INS OBSERVATIONS

In case of sensors carried on satellites the spacecraft trajectories, which are smooth and predictable, can be well described by piecewise polynomial functions. Instead in case of sensors carried on aircraft the direct measurement of the external orientation is indispensable, because the trajectory is unpredictable and the effects of the flight turbulence are not negligible. Nowadays GPS/INS instruments carried on board, together with accurate filtering techniques, provide the sensor external orientation of each image line and allow the estimation of the ground coordinates with forward intersection. Anyway the observations provided by GPS/INS do not refer to the camera PC: the position data refer to a local system centred in the GPS antenna and the attitude refer to a local frame with origin in the INS instrument. These two systems are shifted and rotated with respect to the image one, therefore the collinearity equations (Equations 1 and 3) have to be extended in order to include the offset vectors and the misalignment angles between the image and the GPS and INS frames (Poli, 2002). Anyway the values of the reference systems displacements and rotations are usually not available and additional systematic errors occur in the measurements. In order to solve this problem, the piecewise polynomial functions could be used to model the GPS/INS misalignments and errors. Therefore the proposed sensor model based on this kind of polynomials was modified and extended in order to take into account the GPS/INS observations during the georeferencing of imagery from CCD linear array sensors carried on aircraft.

Supposing that the sensor trajectory is provided for each image line and the scanning time is constant, the functions modelling the sensor external orientation can be considered dependent on the line number, instead of the acquisition time.

The aircraft trajectory is divided into segments. Calling l^i_{ini} and l^i_{fin} the first and last lines of each segment *i* and *l* the processed line number, the variable $\bar{l}$:

$$\bar{l} = \frac{l - l^i_{ini}}{l^i_{fin} - l^i_{ini}} \in [0,1] \tag{14}$$

is defined in each segment.

The trajectory model described in Equation 6 is modified in order to include the GPS/INS observations. The sensor attitude and position of each image line *l* belonging to segment *i* are modelled as the sum of the measured position and attitude data for that line plus the second order polynomial function depending on $\bar{l}$, resulting in:

$$\begin{aligned}
X_C(\bar{l}) &= X_{instr} + X^i_0 + X^i_1\bar{l} + X^i_2\bar{l}^2 \\
Y_C(\bar{l}) &= Y_{instr} + Y^i_0 + Y^i_1\bar{l} + Y^i_2\bar{l}^2 \\
Z_C(\bar{l}) &= Z_{instr} + Z^i_0 + Z^i_1\bar{l} + Z^i_2\bar{l}^2 \\
\omega_C(\bar{l}) &= \omega_{instr} + \omega^i_0 + \omega^i_1\bar{l} + \omega^i_2\bar{l}^2 \\
\varphi_C(\bar{l}) &= \varphi_{instr} + \varphi^i_0 + \varphi^i_1\bar{l} + \varphi^i_2\bar{l}^2 \\
\kappa_C(\bar{l}) &= \kappa_{instr} + \kappa^i_0 + \kappa^i_1\bar{l} + \kappa^i_2\bar{l}^2
\end{aligned} \tag{15}$$

where:

$[X_{instr}\ \ Y_{instr}\ \ Z_{instr}]$: PC position observed with GPS;

$[\omega_{instr}\ \ \varphi_{instr}\ \ \kappa_{instr}]$: PC attitude observed with INS;

$[X_0 X_1 X_2\ \ldots\ \kappa_0 \kappa_1 \kappa_2]^i$: 18 unknown parameters for segment *i*.

The constant terms $(X_0, Y_0, Z_0, \omega_0, \varphi_0, \kappa_0)^i$ correspond to the shifts and angular drifts between the image system and the GPS and INS systems, while the linear and quadratic terms (X_1, Y_1, Z_1, ω_1, φ_1 , κ_1 and X_2, Y_2, Z_2, ω_2, φ_2, $\kappa_2)^i$ model the additional errors in the GPS/INS measurements.

The observations system (Equation 13) is formed combining the collinearity equations (Equations 2 and 4) with the trajectory modelling (Equation 15) and the soft constraints for X_C, Y_C, Z_C, ω_C, φ_C and κ_C (Equations 8, 11, 12). The solution is estimated with least-squares adjustment using the same procedure described in section 3.1. As initial values, the parameters modelling the sensor external orientation (x^0_{EO}) are set equal to zero and the approximate ground coordinates of the TPs (x^0_{TP}) are estimated with forward intersection, using the GPS/INS observations $(X_{instr}, Y_{instr}, Z_{instr}, \omega_{instr}, \varphi_{instr}, \kappa_{instr})_l$ as external orientation.

6. TEST ON TLS

The indirect georeferencing model that integrates the GPS/INS observations in the trajectory modelling was tested on a sensor carried on helicopter with GPS/INS instruments. The sensor is the Japanese TLS (Three-Line Sensor), developed by Starlabo Corporation, Tokyo. It consists of one-lens optical system (focal length: 60.36 mm) and three lines of 10200 elements each (pixel size: 7x7 μm), scanning in forward (+21.5°), nadir and backward (-21.5°) directions (Murai, 2000; Gruen et al., 2002). The internal orientation and the pixels' positions in the focal plane were available from laboratory calibration. The sensor was carried on a helicopter that flew on GSI test area in Japan at a mean height of about 475 m above ground, resulting in a base over height ratio of 0.7 and a footprint of about 6 cm on the ground. The sensor attitude and position for each exposure were available from post-processing of GPS/INS measurements, but without any information about their accuracy. The image and ground coordinates of 47 signalised GCPs were also provided. They were measured in the images with manual matching and on the ground with surveying methods based on GPS. Their distribution is shown in Figure 4, together with the aircraft trajectory. The GCPs coordinates and the helicopter position were provided in a local tangent system.

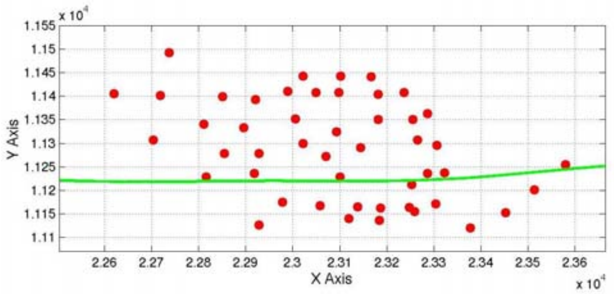

Figure 4. Aircraft trajectory and GCPs distribution in local tangent system.

6.1 Results

Using the available image coordinates of the 47 GCPs, the calibration values and the sensor external orientation parameters, the ground coordinates of the GCPs were estimated with a forward intersection based on one-lens sensors' geometry (Equation 1). The comparison between estimated and corrected coordinates of the GCPs showed large differences, following a systematic behaviour (Poli, 2001). Therefore a correction of the GPS/INS observations was required and the indirect georeferencing model described in chapter 3 was applied. From the 47 available object points, a group of them was used as GCPs and the remaining as TPs. The TPs ground coordinates estimated by the triangulation were compared to their correct values and used for the tests' control. Various combinations of GCPs and TPs were chosen in order to evaluate the influence of the ground information. Table 1 provides a summary of the resulting absolute accuracy in the different test configurations. 6, 12 and 24 GCPs were tested, using 6 and 10 segments for the external orientation modelling. Absolute accuracies in the range 7-13 cm for X, 6-9 cm for Y and 8-16 cm for Z were achieved, corresponding to 1.1-2.1 pixels, 1.0-1.5 pixels and 1.3-2.6 pixels; anyway the errors contained in the image coordinates measured from manual matching could have affected the results. The comparison between the results from the different tests confirms that the triangulation accuracy is influenced by the number and distribution of ground information and improves with the number of GCPs. As far as the modelling functions are concerned, the division of the trajectory in a larger number of segments does not imply any substantial improvements.

The results also confirmed that the original GPS/INS data were not referring to the camera PC, but to the GPS and INS systems. In fact in all test configurations important values for X_0, Y_0, Z_0 and ω_0, φ_0, κ_0 were estimated in all segments. The first and second order terms too were not negligible, showing that systematic errors occurred.

		GCPs+ TPs		
		24+23	12+35	6+41
6 segments	RMS_X	0.076	0.091	0.104
	RMS_Y	0.064	0.083	0.081
	RMS_Z	0.083	0.098	0.085
10 segments	RMS_X	0.078	0.083	0.135
	RMS_Y	0.074	0.064	0.092
	RMS_Z	0.112	0.109	0.165

Table 1. RMS values (in meters) of the estimated TPs coordinates.

7. CONCLUSIONS

A general sensor model for multi-line CCD array sensors with along stereo viewing has been presented. The model combines the classic photogrammetric collinearity equations with the sensor external orientation modelling, resulting in an integrated triangulation. The advantage of the proposed model is that it can be applied both on imagery acquired by sensors carried on satellite and on sensors carried on aircraft with GPS/INS instruments. In the first case, the model estimates directly the sensor external orientation, while with airborne sensors it corrects the observations provided by GPS/INS instruments. In both cases, piecewise polynomial functions are used and the unknown parameters are estimated with least-squares adjustment. The model was tested on MOMS-02 (multi-lens, carried on satellite) and on TLS sensor (1 lens, carried on helicopter), with different GCPs and TPs distributions. An accuracy of 0.2, 0.4 and 0.7 pixels for *X*, *Y* and *Z* was achieved with the MOMS-02 stereo-pair, while for TLS imagery the achieved pixel accuracy was 1.1, 1.0 and 1.3 pixels for *X*, *Y* and *Z*. The first results confirm that the presented indirect georeferencing model can be applied to a wide class of sensors. The results achieved with sensors carried on spacecraft are better than the ones obtained with sensors carried on aircraft, because of the different characteristics of the trajectories. In fact satellites can maintain a smooth and stable orbit during the acquisition of the images, while the aircraft trajectories are unpredictable and influenced by atmospheric turbulence. Therefore, as future work, the current algorithms will be further investigated and tested. Moreover self-calibration process will be analysed and other trajectory modelling functions will be studied.

8. ACKNOWLEDGEMENTS

This work is part of Cloudmap2 project, funded by the European Commission under the Fifth Framework program for Energy, Environment and Sustainable Development.
Special thanks are addressed to Starlabo Corporation, Tokyo who allowed the publication of TLS results and to Manfred Lehner, from DLR, for his contribution for the MOMS-02 dataset.

9. REFERENCES

Chen, T., 2001. High precision georeference for airborne Three-Line Scanner (TLS) imagery. *Proceedings of 3rd International Image Sensing Seminar on New Development in Digital Photogrammetry, Gifu, Japan*, pp. 71-82.

Cramer, M., Stallmann, D., Haala, N., 2000. Direct georeferencing using GPS/INS exterior orientations for photogrammetric applications. *International Archives of Photogrammetry and Remote Sensing*, Vol. 33, Part B3, Amsterdam, pp. 198-205.

Ebner, H., Kornus, W., Ohlhof, T., 1992. A simulation study on point determination for the MOMS-02/D2 space project using an extended functional model. *International Archives of Photogrammetry and Remote Sensing*, Vol. 29, Part B4, Washington D.C., pp. 458-464.

Gruen, A., Zhang L., 2002. Sensor modeling for aerial mobile mapping with Three-Line-Scanner (TLS) imagery. *International Archives of Photogrammetry and Remote Sensing*, Vol. 34, Part 2, Xi'an (in press).

Haala, N., Stallmann, D., Cramer, M., 1998. Calibration of directly measured position and attitude by aerotriangulation of three-line airborne imagery. *Proceedings of ISPRS Commission III Symposium on Object Recognition and Scene Classifications from Multispectral and Multisensor Pixels, Ohio*, pp. 28-30.

Kornus, W., 1998. Dreidimensionale Objektrekonstruktion mit digitalen Dreizeilenscannerdaten des Weltraumprojekts MOM-02/D2. *DLR-Forschungsbericht* 97-54 (in German).

Kratky, V., 1989. Rigorous photogrammetric processing of SPOT images at CCM Canada. *ISPRS Journal of Photogrammetry and Remote Sensing*, No. 44, pp. 53-71.

Lee, C., Theiss, H.J., Bethel, J.S., Mikhail, E.M., 2000. Rigorous mathematical modeling of airborne pushbroom imaging systems. *Photogrammetric Engineering & Remote Sensing*, Vol. 66, No. 4, pp. 385-392.

Mostafa, M.M.R., Schwarz, K., 2000. A multi-sensor system for airborne image capture and georeferencing. *Photogrammetric Engineering & Remote Sensing*, Vol. 66, No. 12, pp. 1417-1423.

Murai, S., Matsumoto, Y., 2000. The development of airborne three line scanner with high accuracy INS and GPS for analysing car velocity distribution. *International Archives of Photogrammetry and Remote Sensing*, Vol. 33, Part B2, Amsterdam, pp. 416-421.

Poli, D., 2001. Direct georeferencing of multi-line images with a general sensor model. ISPRS Workshop "High resolution mapping from space 2001", 18-21 September 2001, Hannover. Proceedings on CD.

Poli, D., 2002. Indirect georeferencing of airborne multi-line array sensors: a simulated case study. *International Archives of Photogrammetry and Remote Sensing*, Vol. 34, Part 3, Graz (in press).

Tempelmann, U., Boerner, A., Chaplin, B., Hinsken, L., Mykhalevych, B., Miller, S., Recke, U., Reulke, R., Uebbing, R., 2000. Photogrammetric software for the LH systems ADS40. *International Archives of Photogrammetry and Remote Sensing*, Vol. 33, Part B2, Amsterdam, pp. 552-559.